AIP | Journal of Applied Physics

Dispersion of the linear and nonlinear optical susceptibilities of the CuAl(S1xSex)2 mixed chaclcopyrite compounds

A. H. Reshak, M. G. Brik, and S. Auluck

Citation: Journal of Applied Physics **116**, 103501 (2014); doi: 10.1063/1.4894829
View online: http://dx.doi.org/10.1063/1.4894829
View Table of Contents: http://scitation.aip.org/content/aip/journal/jap/116/10?ver=pdfcov
Published by the AIP Publishing

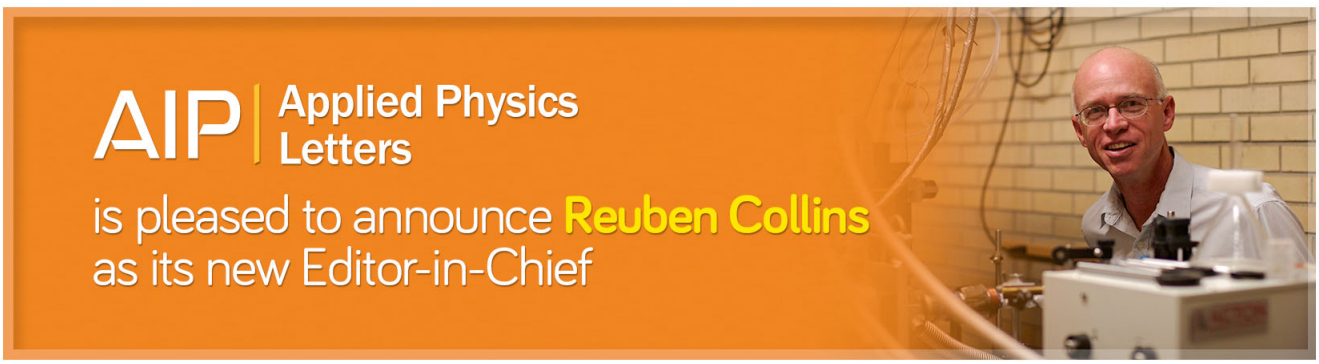

Dispersion of the linear and nonlinear optical susceptibilities of the $CuAl(S_{1-x}Se_x)_2$ mixed chaclcopyrite compounds

A. H. Reshak,[1,2,a)] M. G. Brik,[3,4] and S. Auluck[5]
[1]*New Technologies - Research Centre, University of West Bohemia, Univerzitni 8, 306 14 Pilsen, Czech Republic*
[2]*Center of Excellence Geopolymer and Green Technology, School of Material Engineering, University Malaysia Perlis, 01007 Kangar, Perlis, Malaysia*
[3]*College of Mathematics and Physics, Chongqing University of Posts and Telecommunications, Chongqing 400065, People's Republic of China*
[4]*Institute of Physics, University of Tartu, Ravila 14C, Tartu 50411, Estonia*
[5]*Council of Scientific and Industrial Research—National Physical Laboratory Dr. K S Krishnan Marg, New Delhi 110012, India*

(Received 31 July 2014; accepted 26 August 2014; published online 8 September 2014)

Based on the electronic band structure, we have calculated the dispersion of the linear and nonlinear optical susceptibilities for the mixed $CuAl(S_{1-x}Se_x)_2$ chaclcopyrite compounds with $x = 0.0$, 0.25, 0.5, 0.75, and 1.0. Calculations are performed within the Perdew-Becke-Ernzerhof general gradient approximation. The investigated compounds possess a direct band gap of about 2.2 eV ($CuAlS_2$), 1.9 eV ($CuAl(S_{0.75}Se_{0.25})_2$), 1.7 eV ($CuAl(S_{0.5}Se_{0.5})_2$), 1.5 eV ($CuAl(S_{0.25}Se_{0.75})_2$), and 1.4 eV ($CuAlSe_2$) which tuned to make them optically active for the optoelectronics and photovoltaic applications. These results confirm that substituting S by Se causes significant band gaps' reduction. The optical function's dispersion $\varepsilon_2^{xx}(\omega)$ and $\varepsilon_2^{zz}(\omega)/\varepsilon_2^{xx}(\omega)$, $\varepsilon_2^{yy}(\omega)$, and $\varepsilon_2^{zz}(\omega)$ was calculated and discussed in detail. To demonstrate the effect of substituting S by Se on the complex second-order nonlinear optical susceptibility tensors, we performed detailed calculations for the complex second-order nonlinear optical susceptibility tensors, which show that the neat parents compounds $CuAlS_2$ and $CuAlSe_2$ exhibit $|\chi^{(2)}_{123}(-2\omega;\omega;\omega)|$ as the dominant component, while the mixed alloys exhibit $|\chi^{(2)}_{111}(-2\omega;\omega;\omega)|$ as the dominant component. The features of $|\chi^{(2)}_{123}(-2\omega;\omega;\omega)|$ and $|\chi^{(2)}_{111}(-2\omega;\omega;\omega)|$ spectra were analyzed on the basis of the absorptive part of the corresponding dielectric function $\varepsilon_2(\omega)$ as a function of both $\omega/2$ and ω. © *2014 AIP Publishing LLC*.
[http://dx.doi.org/10.1063/1.4894829]

I. INTRODUCTION

In the last decade, the density functional theory (DFT)-based first-principles calculations have been successfully used to obtain different properties of materials. The structural parameters and dynamical properties of crystals determine a wide range of microscopic and macroscopic behavior: diffraction, sound velocity, elastic constants, Raman and infrared (IR) absorption, inelastic neutron scattering, specific heat, etc. The ternary $A^IB^{III}C_2^{VI}$ semiconducting compounds which crystallize in the chalcopyrite structure have received much attention in the recent years.[1–7] They form a large group of semiconducting materials with diverse optical, electrical, and structural properties.[8–15] Ternary chalcopyrite compounds with suitable band gaps appear to be promising candidates for various applications, such as solar-cell materials,[16] light-emitting diodes,[17] nonlinear optics,[18] and optical frequency conversion applications in all solid state based tunable laser systems.[19] These have potentially significant advantages over dye lasers because of their easier operation and the potential for more compact devices. Tunable frequency conversion in the mid-IR is based on the optical parametric oscillators (OPOs) using pump lasers in the near IR.[19] On the other hand, the frequency doubling devices also allow one to expand the range of powerful lasers from the far IR, such as the CO_2 lasers to the mid-infrared.[19–21]

The birefringence parameters are important for the above-mentioned applications. As far as the chalcopyrite compounds are concerned, $CuInTe_2$ and $AgGaTe_2$ have a positive birefringence, whereas $CuInS_2$, $CuInSe_2$, $AgGaS_2$, and $AgGaSe_2$ are characterized by a negative one.[22–24] $AgGaS_2$ is mostly in use as a near infrared pumped OPO.[19] Further the range of transparency of $AgGaSe_2$ in the infrared allows for its use as an efficient frequency doubler and tripler of the CO_2 laser lines.[19]

The specific $A^{XI}B^{XIII}C_2^{XVI}$ chalcopyrites concerned in this work used copper as the group *XI* element, aluminum as the group *XIII* element, and sulfur or selenium as the group *XVI* element (the standard group numbering of the chemical elements in the periodic table is used, as recommended by the International Union of Pure and Applied Chemistry (IUPAC)). Since these compounds display large birefringence,[25–28] they are potentially interesting as nonlinear optical materials, as well as semiconductors, whose band gap favors their applications for solar energetic. So far, however, the trends of the coupling coefficients in these materials are

a)Author to whom correspondence should be addressed. Electronic mail: maalidph@yahoo.com. Tel. +420 777729583.

not well understood for neat materials and mixed compounds with the chalcopyrite structure. Here, the first-principle calculations are used to predict enhancement of $\chi^{(2)}(\omega)$ by substitution of S by Se when moving from $CuAlS_2$ to $CuAlSe_2$ in the whole range of the anion's concentration.

Since the band structure of $A^{XI}B^{XIII}C_2^{XVI}$ chalcopyrites is influenced by intrinsic defects which form additional trapping levels within the band gap of the host materials, this leads to an enhancement of the optical properties. As a result, the material's properties can be tuned to make them suitable for the optoelectronics and photovoltaic applications. Therefore, further insight into the electronic structure can be obtained from the careful analysis of the optical properties, with an emphasis on the influence of concentration on the variation of the studied characteristics. We would like to mention that we are not aware of calculations or experimental data for the nonlinear optical susceptibilities for the mixed $CuAl(S_{1-x}Se_x)_2$ compounds. Since these materials are technologically important and are widely used for solar cell, optoelectronics, and photovoltaic applications, we thought it worthwhile to investigate them further and calculate their linear and nonlinear optical properties.

II. DETAILS OF CALCULATIONS

$CuAl(S_{1-x}Se_x)_2$ belongs to the group of ternary semiconducting compounds which are of great interest as nonlinear optical materials.[29,30] The crystal structure of $CuAl(S_{1-x}Se_x)_2$ for x = 0.0, 0.25, 0.5, 0.75, and 1.0, is shown in Fig. 1. As the first step of our analysis, we optimized the crystal structure of the $CuAl(S_{1-x}Se_x)_2$ compounds using the CASTEP module[31] of Materials Studio. The calculated lattice constants for $CuAlS_2$ (a = 5.2868 Å, c = 10.4268 Å), $CuAl(S_{0.75}Se_{0.25})_2$ (a = 5.3655 Å, c = 10.5652 Å), $CuAl(S_{0.5}Se_{0.5})_2$ (a = 5.4449 Å, c = 10.7171 Å), $CuAl(S_{0.25}Se_{0.75})_2$ (a = 5.5278 Å, c = 10.8398 Å), and $CuAlSe_2$ (a = 5.5559 Å, c = 11.0291 Å) show very good agreement with the available experimental data for $CuAlS_2$ (a = 5.3336 Å, c = 10.4440 Å),[32] $CuAl(S_{0.5}Se_{0.5})_2$ (a = 5.46 Å, c = 10.67 Å),[33] and $CuAlSe_2$ (a = 5.606 Å, c = 10.90 Å).[34]

The exchange-correlation effects were modelled within the generalized gradient approximation (GGA) with the Perdew-Burke-Ernzerhof (PBE) functional.[35] The plane wave basis set cut-off energy was set at 290 eV, the Monkhorst-Pack scheme k-point grid sampling was

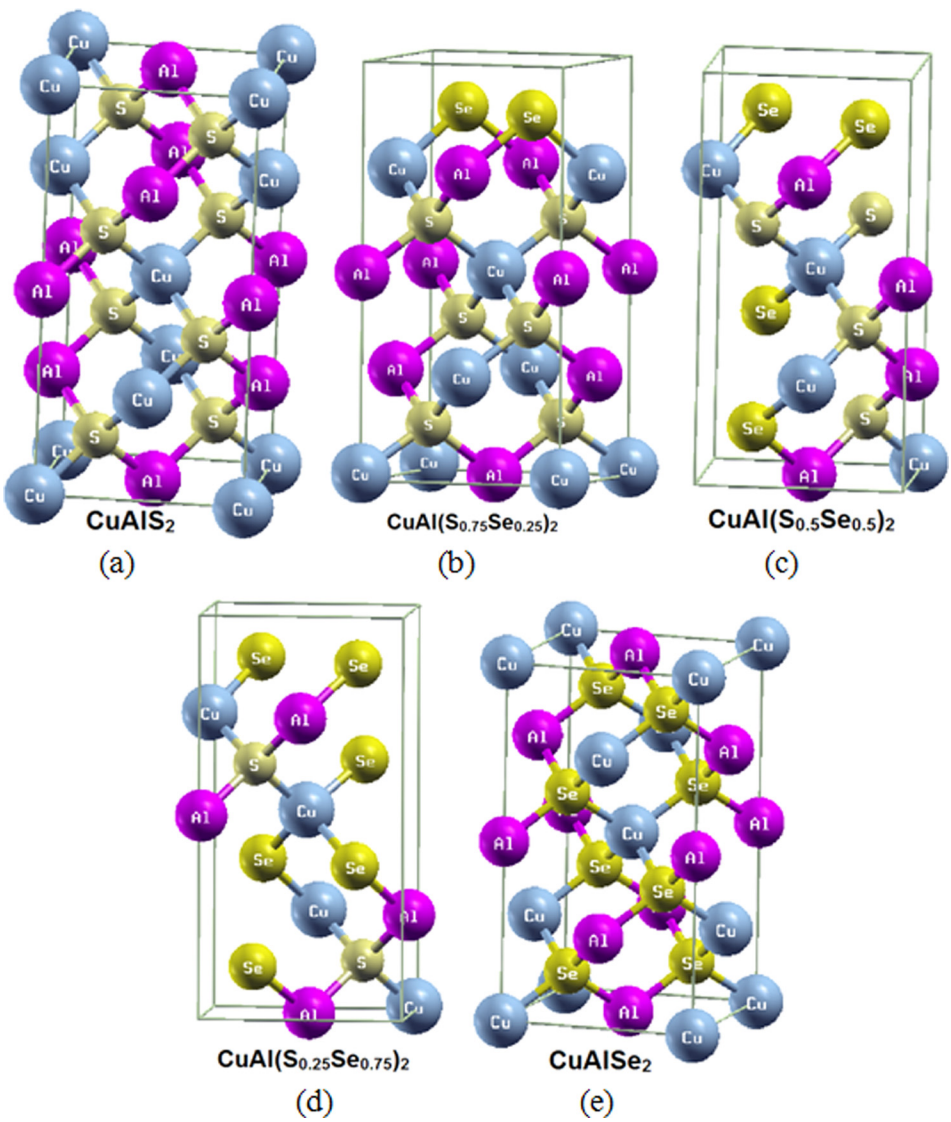

FIG. 1. Fragment of the crystal structure of $CuAl(S_{1-x}Se_x)_2$ with x = 0.0, 0.25, 0.5, 0.75, and 1.0.

$5 \times 5 \times 3$ k-points for the Brillouin zone. The calculations were repeated until the following convergence tolerance parameters were achieved: energy 10^{-5} eV/atom, maximal force and stress 0.03 eV/Å and 0.05 GPa, respectively, the maximal displacement 0.001 Å. The compositional dependence of the calculated properties was studied by gradual replacement of the S atoms in the $CuAlS_2$ unit cell by the Se atoms, corresponding to the Se concentration (in %) of 0, 25, 50, 75, and 100. The considered electronic configurations were $3d^{10}4s^1$ for Cu, $3s^23p^1$ for Al, $3s^23p^4$ for S, and $4s^24p^4$ for Se. All obtained results are described and discussed in Sec. III. Since the calculations of the nonlinear optical properties are impossible in CASTEP, in the next step we used the state-of-the-art full potential linear augmented plane wave (FPLAPW) method in a scalar relativistic version as embodied in the WIEN2k code.[36] This is an implementation of the DFT. Exchange and correlation potential was described by the GGA of PBE, which is based on exchange-correlation energy optimization to calculate the total energy. The structure was optimized by minimization of the forces (1 mRy/au) acting on the atoms using Perdew-Becke-Ernzerhof general gradient approximation (PBE-GGA). The Kohn-Sham equations are solved using a basis of linear APWs. The potential and charge density in the muffin-tin (MT) spheres are expanded in spherical harmonics with $l_{max} = 8$ and nonspherical components up to $l_{max} = 6$. In the interstitial region, the potential and the charge density are represented by Fourier series. Self-consistency is obtained using 400 $\vec{k}$ points in the irreducible Brillouin zone (IBZ) for $x = 0.0$ and 1.0, while for $x = 0.25$, 0.5, and 0.75, a mish of 600 $\vec{k}$ points was used. We have calculated the linear optical susceptibilities using 800 $\vec{k}$ points and the nonlinear optical susceptibilities using 1600 $\vec{k}$ points in the IBZ.

III. RESULTS AND DISCUSSION

A. Salient feature of the electronic band structures

It is interesting that the $CuAlX_2$ ($X = S$, Se, Te) compounds possess a direct band gap which makes these materials optically active. The energy band gap values along with the experimental values and the previous theoretical results[37] are listed in Table I. We should emphasize that the energy band gap values are less than the experimental data which are in the limit of the DFT. We find that the effect of substituting S by Se causes to push the conduction band maximum (CBM) towards Fermi level (E_F) resulting in reduction of the energy band gap which has significant influence on the optical properties.

B. Linear optical properties

The compounds, $CuAlS_2$ and $CuAlSe_2$, crystallize in the non-centro-symmetric tetragonal space group I-42d, whereas $CuAl(S_{0.75}Se_{0.25})_2$, $CuAl(S_{0.5}Se_{0.5})_2$, and $CuAl(S_{0.25}Se_{0.75})_2$ crystallize in triclinic space group (P-1). These symmetries allow two/three non-zero components of the second-order dielectric (optical) tensor corresponding to the electric field $\vec{E}$ being directed along **a**, **b**, and **c**-crystallographic axes (which they identify as *x, y,* and *z*). These compounds possess pronounced structures of the two/three principal complex tensor components. The imaginary part of the two/three principal complex tensor components completely defines the linear optical susceptibilities. The imaginary parts $\varepsilon_2^{xx}(\omega)$ and $\varepsilon_2^{zz}(\omega)/\varepsilon_2^{xx}(\omega)$, $\varepsilon_2^{yy}(\omega)$, and $\varepsilon_2^{zz}(\omega)$ of the optical function's dispersion were calculated using expression given somewhere else.[38]

To overcome the drawback of the DFT calculation (band gap underestimation), we have applied the scissors correction to the optical properties in order to bring the value of the calculated energy gap exactly to the measured gap. The scissors correction is the difference between the calculated and measured energy gaps. We find that the effect of replacing S by Se has significant influence on the energy gap. Thus, we expect that the effect on the optical properties will be significant. The calculated optical function's dispersion was illustrated in Figs. 2(a)–2(e). The electronic band structure of the investigated compound suggests that the first spectral structure in $\varepsilon_2^{xx}(\omega)$ and $\varepsilon_2^{zz}(\omega)/\varepsilon_2^{xx}(\omega)$, $\varepsilon_2^{yy}(\omega)$, and $\varepsilon_2^{zz}(\omega)$ is due to the transition from Cu-s/p/d, Al-s/p, and S/Se-p to Cu-s/p, Al-p, and S/Se-p states. The second structure

TABLE I. The calculated energy band gap in comparison with the previous theoretical results and the experimental value, $\varepsilon_1^{xx}(0)$, $\varepsilon_1^{yy}(0)$, $\varepsilon_1^{zz}(0)$, $n^{xx}(0)$, $n^{yy}(0)$, $n^{zz}(0)$, and $\Delta n(0)$.

	$CuAlS_2$	$CuAl(S_{0.75}Se_{0.25})_2$	$CuAl(S_{0.5}Se_{0.5})_2$	$CuAl(S_{0.25}Se_{0.75})_2$	$CuAlSe_2$
Eg (eV)	2.2[a], 1.93[b], 1.89[b], 3.50[c]	1.9[a]	1.7[a]	1.5[a]	1.4[a], 1.14[b], 1.02[b], 2.67[d]
$\varepsilon_1^{xx}(0)$	7.13[a]	7.45[a]	7.78[a]	8.08[a]	8.26[a]
$\varepsilon_1^{yy}(0)$	…	7.40[a]	7.72[a]	8.03[a]	…
$\varepsilon_1^{zz}(0)$	7.07[a]	7.40[a]	7.71[a]	8.03[a]	7.60[a]
$n^{xx}(0)$ ($n^{xx}(\omega)$)	2.670 (2.740)	2.730 (2.805)	2.789 (2.874)	2.842 (2.943)	2.880 (2.960)
$n^{yy}(0)$ ($n^{yy}(\omega)$)	…	2.720 (2.790)	2.779 (2.862)	2.834 (2.931)	…
$n^{zz}(0)$ ($n^{zz}(\omega)$)	2.660 (2.720)	2.720 (2.795)	2.777 (2.866)	2.834 (2.942)	2.760 (2.840)
$n(\omega)$ exp	2.378[e]	…	…	…	2.492[e], 2.600[f]
$\Delta n(0)$ ($\Delta n(\omega)$)	0.010 (0.020)	−0.010(−0.0125)	0.011 (0.010)	0.002 (0.0065)	0.12 (0.12)

[a]This work.
[b]Ref. 37.
[c]Ref. 45 (experimental).
[d]Ref. 2 (experimental).
[e]Ref. 41 (experimental).
[f]Ref. 42 (experimental).

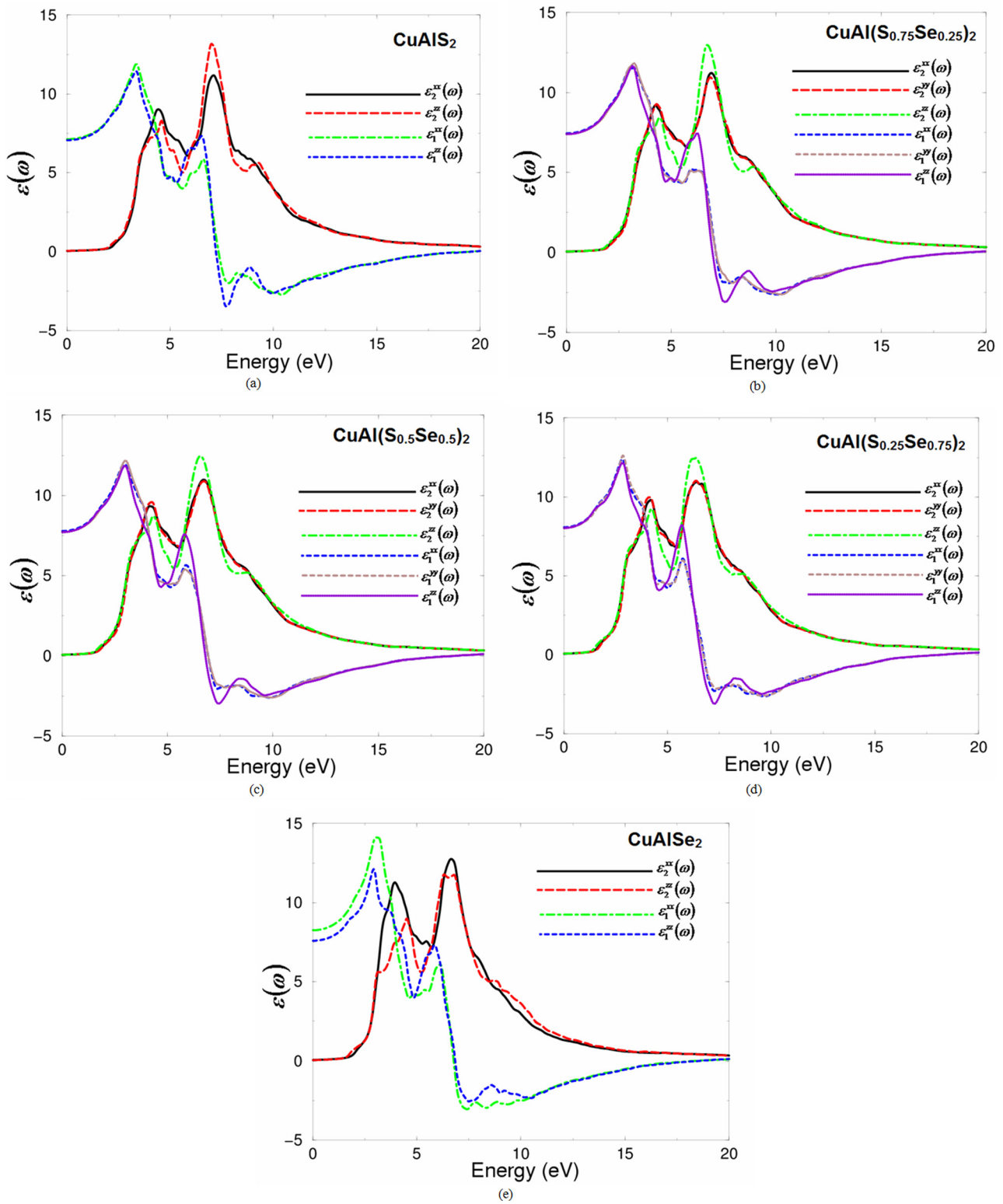

FIG. 2. (a) Calculated $\varepsilon_2^{xx}(\omega)$ and $\varepsilon_2^{zz}(\omega)/\varepsilon_2^{xx}(\omega)$, $\varepsilon_2^{yy}(\omega)$, $\varepsilon_2^{zz}(\omega)$ and $\varepsilon_1^{xx}(\omega)$ and $\varepsilon_1^{zz}(\omega)/\varepsilon_1^{xx}(\omega)$, $\varepsilon_1^{yy}(\omega)$, $\varepsilon_1^{zz}(\omega)$ for $CuAl(S_{1-x}Se_x)_2$ with x = 0.0, 0.25, 0.5, 0.75, and 1.0.

corresponds to transition between Cu-s/p/d, Al-s, and S/Se-p to Cu-s/d, Al-s/p, and S/Se-p states. The optical absorption edge (threshold) for $\varepsilon_2^{xx}(\omega)$ and $\varepsilon_2^{zz}(\omega)/\varepsilon_2^{xx}(\omega)$, $\varepsilon_2^{yy}(\omega)$, and $\varepsilon_2^{zz}(\omega)$ varies between 2.2 and 1.4 eV (see Figs. 2(a)–2(e)). We find that all the structures of $\varepsilon_2^{xx}(\omega)$ and $\varepsilon_2^{zz}(\omega)/\varepsilon_2^{xx}(\omega)$, $\varepsilon_2^{yy}(\omega)$, and $\varepsilon_2^{zz}(\omega)$, are shifted to lower energies with substituting S by Se. There exists anisotropy between the principal complex tensor components. We should emphasize that the anisotropy in the linear optical susceptibilities favors an enhanced phase matching conditions necessary for observation of the second harmonic generation (SHG) and optical parametric oscillation. The real part $\varepsilon_1^{xx}(\omega)$ and $\varepsilon_1^{zz}(\omega)/\varepsilon_1^{xx}(\omega)$, $\varepsilon_1^{yy}(\omega)$, and $\varepsilon_1^{zz}(\omega)$ of the corresponding principle complex tensor components (see Figs. 2(a)–2(e)) are obtained from the imaginary part of these

principal complex tensor components by means of the Kramers-Kronig transformation.[39] The values of $\varepsilon_1^{xx}(0)$, $\varepsilon_1^{yy}(0)$, and $\varepsilon_1^{zz}(0)$ are presented in Table I. Following Table I, it is clear that the larger $\varepsilon_1(0)$ value belongs to the smaller energy gap. This could be explained on the basis of the Penn model.[40] Penn proposed a relation between $\varepsilon(0)$ and E_g, $\varepsilon(0) \approx 1 + (\hbar\omega_P/E_g)^2$. E_g is some kind of averaged energy gap which could be related to the real energy gap. It is clear that $\varepsilon(0)$ is inversely proportional with E_g.

We have calculated the refraction indices at static limit and at $\lambda = 1064$ nm (1.165 eV), these values are listed in Table I along with the experimental data.[41,42] The birefringence is the difference between the extraordinary and ordinary refraction indices, $\Delta n(\omega) = n_e(\omega) - n_o(\omega)$, where $n_o(\omega)$ is the index of refraction for an electric field oriented along the **c**-axis and $n_e(\omega)$ is the index of refraction for an electric field perpendicular to the **c**-axis. It is clear that the birefringence is crucial only in the non-absorbing spectral

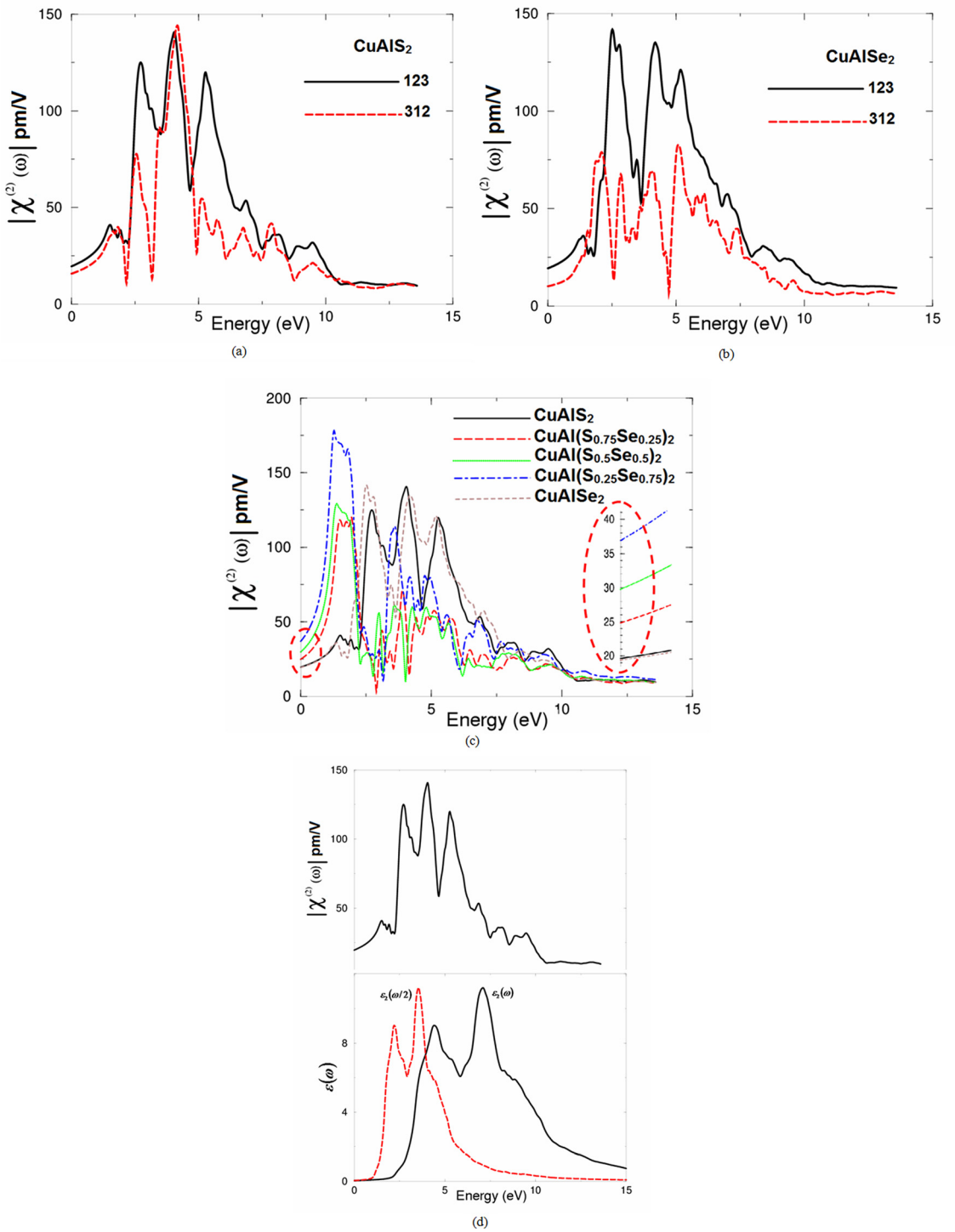

FIG. 3. (a) and (b) Calculated $|\chi^{(2)}_{123}(\omega)|$ and $|\chi^{(2)}_{312}(\omega)|$ for $CuAl(S_{1-x}Se_x)_2$ with x = 0.0 and 1.0. (c) Calculated $|\chi^{(2)}_{123}(\omega)|$ and $|\chi^{(2)}_{111}(\omega)|$ for $CuAl(S_{1-x}Se_x)_2$ with x = 0.0, 0.25, 0.5, 0.75, and 1.0. (d)—*upper panel*—Calculated $|\chi^{(2)}_{123}(\omega)|$ (dark solid curve—black line); *lower panel*—calculated $\varepsilon_2^{xx}(\omega)$ (dark solid curve—black line); calculated $\varepsilon_2^{xx}(\omega/2)$ (dark dashed curve—red line).

TABLE II. Calculated $|\chi^{(2)}_{ijk}(\omega)|$ in pm/V at static limit and at $\lambda = 1064$ nm.

Compound	Tensor components	Theory $\chi^{(2)}_{ijk}(\omega)$ at static limit in (pm/V)	Theory $\chi^{(2)}_{ijk}(\omega)$ at $\lambda = 1064$ nm in (pm/V)
$CuAlS_2$	$\|\chi^{(2)}_{123}(\omega)\|$	19.7	31.0
$CuAl(S_{0.75}Se_{0.25})_2$	$\|\chi^{(2)}_{111}(\omega)\|$	25.0	68.0
$CuAl(S_{0.5}Se_{0.5})_2$	$\|\chi^{(2)}_{111}(\omega)\|$	30.0	97.0
$CuAl(S_{0.25}Se_{0.75})_2$	$\|\chi^{(2)}_{111}(\omega)\|$	37.0	156.0
$CuAlSe_2$	$\|\chi^{(2)}_{123}(\omega)\|$	19.8	33.0

range, which is below the energy gap. We have found that these materials possess positive birefringence at static limit and at $\lambda = 1064$ nm (1.165 eV), see Table I.

C. SHG

The space group I-42d allows only two nonzero complex second-order nonlinear optical susceptibility tensors $\chi^{(2)}_{123}(-2\omega;\omega;\omega)$, $\chi^{(2)}_{312}(-2\omega;\omega;\omega)$, whereas for the space group (P-1), all elements are independent and nonzero. Following Figs. 3(a)–3(c), it is clear that $|\chi^{(2)}_{123}(-2\omega;\omega;\omega)|$ is the dominant component for the space group I-42d ($CuAlS_2$ and $CuAlSe_2$). While $|\chi^{(2)}_{111}(-2\omega;\omega;\omega)|$ is the dominant component for the space group P-1 ($CuAl(S_{0.75}Se_{0.25})_2$, $CuAl(S_{0.5}Se_{0.5})_2$ and $CuAl(S_{0.25}Se_{0.75})_2$. To avoid the DFT's drawback, we consider the quasi-particle self-energy corrections at the level of scissors operators in which the energy bands are rigidly shifted to merely bring the calculated energy gap closer to the experimental gap. We have calculated $|\chi^{(2)}_{123}(-2\omega;\omega;\omega)|$ and $|\chi^{(2)}_{111}(-2\omega;\omega;\omega)|$ at $\lambda = 1064$ nm and at static limit $|\chi^{(2)}_{123}(0)|$ and $|\chi^{(2)}_{111}(0)|$. These values are listed in Table II. The static values of the second order susceptibility tensor are very important and can be used to estimate their relative SHG efficiency. The complex second-order nonlinear optical susceptibility tensors are zero below $E_g/2$ and slowly increases up after $E_g/2$ since the 2 ω resonance begin to contribute at energies above $E_g/2$.[43,44] The ω resonance begins to contribute for energy values above E_g. At the spectral range below $E_g/2$, the SHG is dominated by the 2 ω contributions, while above E_g, the major contribution comes from the ω term.

To analyze the features of $|\chi^{(2)}_{123}(-2\omega;\omega;\omega)|$ and $|\chi^{(2)}_{111}(-2\omega;\omega;\omega)|$ spectra, we compare them with the absorptive part of the corresponding dielectric function $\varepsilon_2(\omega)$ as a function of both $\omega/2$ and ω. As prototype, we demonstrate the comparison of $|\chi^{(2)}_{123}(-2\omega;\omega;\omega)|$ with $\varepsilon_2(\omega)$ and $\varepsilon_2(\omega/2)$ of $CuAlS_2$ as illustrated in Fig. 3(d). The first structure in $|\chi^{(2)}_{123}(-2\omega;\omega;\omega)|$ spectra between 1.7 and 4.0 eV is mainly originated from 2 ω resonance. The second structure between 4.0 and 8.0 eV is associated with interference between 2 ω and ω resonances. The last spectral structure which extended from 8.0 eV to 14.0 eV, is mainly due to ω resonance.

IV. CONCLUSIONS

The structural, electronic, linear, and non-linear optical properties of a series of the mixed chalcopyrite semiconducting materials $CuAlS_2$, $CuAlSe_2$, $CuAl(S_{0.75}Se_{0.25})_2$, $CuAl(S_{0.5}Se_{0.5})_2$, and $CuAl(S_{0.25}Se_{0.75})_2$ were calculated. The dispersion of the linear and nonlinear optical susceptibilities for all above-mentioned compounds based on the electronic band structure was obtained. The all electron FPLAPW method with GGA-PBE was employed. The calculated electronic band structure suggested that these materials possess a direct energy band gap. Substituting S by Se cause to push the CBM towards Fermi level resulting in significant band gap reduction from 2.2 to 1.4 eV; such a behavior correlates with a corresponding increase in the lattice constant upon this substitution. The DFT's underestimation of the energy gap was corrected at the level of scissors operators. The calculated optical function's dispersion $\varepsilon_2^{xx}(\omega)$ and $\varepsilon_2^{zz}(\omega)/\varepsilon_2^{xx}(\omega)$, $\varepsilon_2^{yy}(\omega)$, and $\varepsilon_2^{zz}(\omega)$ suggested that the anisotropy exists between the principal complex tensor components. Also, we have calculated the complex second-order nonlinear optical susceptibility tensors, namely, SHG to demonstrate the effect of substituting S by Se on the SHG of the optical susceptibilities. We have analyzed the results and found that the parents' compounds exhibit $|\chi^{(2)}_{333}(\omega)|$ as dominant component, while the alloys exhibit $|\chi^{(2)}_{111}(\omega)|$ as dominant component.

ACKNOWLEDGMENTS

The result was developed within the CENTEM project, Reg. No. CZ.1.05/2.1.00/03.0088, co-funded by the ERDF as part of the Ministry of Education, Youth and Sports OP RDI program. Computational resources were provided by MetaCentrum (LM2010005) and CERIT-SC (CZ.1.05/3.2.00/08.0144) infrastructures. S.A. thanks Council of Scientific and Industrial Research (CSIR)—National Physical Laboratory for financial support. M.G.B. appreciates the financial support from the European Social Fund's Doctoral Studies and Internationalisation Programme DoRa and Ministry of Education and Research of Estonia, project PUT430.

[1]*Ternary and Multinary Compounds*, edited by S. K. Deb and A. Zunger (Materials Research Society, Pittsburgh, PA, 1987).
[2]G. E. Jaffe and A. Zunger, Phys. Rev. B **28**, 5822 (1983); **29**, 1882 (1984).
[3]C. Rincon and C. Bellabarba, Phys. Rev. B **33**, 7160 (1986).
[4]V. Kumar, B. P. Singh, and B. P. Pandey, Comput. Mater. Sci. **87**, 227–231 (2014).
[5]V. Kumar and S. K. Tripathy, J. Alloys Compd. **582**, 101–107 (2014).
[6]V. Kumar, S. K. Tripathy, and V. Jha, Appl. Phys. Lett. **101**(19), 192105 (2012).
[7]V. Kumar, Phys. Chem. Solids **48**, 827 (1987).
[8]E. Parthe, *Crystal Chemistry of Tetrahedral Structures* (Gordon and Breach, New York, 1964).
[9]N. A. Goryunova, *The Chemistry of Diamond-Like Semiconductors* (Chapman and Hall, New York, 1965).
[10]J. L. Shay and J. H. Wernick, *Ternary Chalcopyrite Semiconductors: Growth, Electronic properties and Applications* (Pergamon, Oxford, 1974).

[11]U. Kaufmann and J. Schneider, in *Festkorperprobleme XIV*, edited by J. Treusch (Vieweg, Braunschweig, 1974), p. 229.
[12]J. Wagner, in *Electroluminescence*, edited by J. O. Pankove (Springer, Berlin, 1977), p. 171.
[13]A. Mackinnon, in *Festkorperprobleme XXI*, edited by J. Treusch (Vieweg Dortmund, 1981), p. 149.
[14]A. Miller, A. Mackinnon, and D. Weaire, in *Solid State Physics*, edited by H. Ehrenreich, F. Seitz, and D. Turubull (Academic, New York, 1981), Vol. 36.
[15]B. R. Pamplin, T. Kiyosawa, and K. Mastumoto, Prog. Cryst. Growth Charact. **1**, 331 (1979).
[16]L. L. Kazmerski, Nuovo Cimento D **2**, 2013 (1983).
[17]J. L. Shay, L. M. Schiavone, E. Buehier, and J. H. Wernick, J. Appl. Phys. **43**, 2805 (1972); S. Wagner, J. L. Shay, B. Tell, and H. M. Kasper, Appl. Phys. Lett. **22**, 351 (1973).
[18]B. F. Levine, Phys. Rev. B **7**, 2600 (1973) and references therein.
[19]F. K. Hopkius, Laser Focus World **31**, 87 (1995).
[20]G. C. Catella and D. Burlage, MRS Bull. **23**, 28 (1998).
[21]S. N. Rashkeev and W. R. L. Lambrecht, Phys. Rev. B **63**, 165212 (2001).
[22]S. N. Rashkeev and W. R. Lambrecht, Appl. Phys. Lett. **77**, 190 (2000).
[23]A. MacKinnon, Landolt-Börnstein Numerical Data and Functional Relationships in Science and Technology, New Series, Group III, *Crystal Solid State Physics Vol. 17, Semiconductors, Subvolume h, Physics of Ternary Compounds*, edited by O. Madelung (Springer, Berlin, 1985).
[24]A. S. Borshchevskii, V. S. Grigoréva, Yu. K. Undalov, and T. P. Upatova, Fiz. Tekh. Poluprovodn. **6**, 396 (1972) [Sov. Phys. Semicond. **6**, 338 (1972); Semiconductor **4**, 494 (1970)].
[25]A. H. Reshak, S. Auluck, D. Stys, I. V. Kityk, H. Kamarudin, J. Berdowskie, and Z. Tylczynski, J. Mater. Chem. **21**, 17219 (2011).
[26]A. H. Reshak, V. Kityk, and S. Auluck, J. Phys. Chem. B **114**, 16705–16712 (2010).
[27]A. H. Reshak, S. Auluck, and I. V. Kityk, J. Solid State Chem. **181**, 789–795 (2008).
[28]A. H. Reshak, S. Auluck, and I. V. Kityk, J. Phys.: Condens. Matter **20**, 145209 (2008).
[29]G. D. Boyd, H. Kasper, and J. H. McFee, IEEE J. Quantum Electron. **7**, 563 (1971).
[30]D. S. Chemla, P. J. Kupcek, D. S. Robertson, and R. C. Smith, Opt. Commun. **3**, 29 (1971).
[31]S. J. Clark, M. D. Segall, C. J. Pickard, P. J. Hasnip, M. J. Probert, K. Refson, and M. C. Payne, Z. Kristallogr. **220**, 567–570 (2005).
[32]G. Brandt, A. Rauber, and J. Schneider, J. Solid State Commun. **12**, 481 (1973).
[33]C.-H. Ho and C.-C. Pan, Opt. Express **3**, 480 (2013).
[34]H. Hahn, G. Frank, W. Klingler, A. D. Meyer, and G. Z. Stoerger, Anorg. Allg. Chem. **271**, 153 (1953).
[35]J. P. Perdew, K. Burke, and M. Ernzerhof, Phys. Rev. Lett. **77**, 3865 (1996).
[36]P. Blaha, K. Schwarz, G. K. H. Madsen, D. Kvasnicka, and J. Luitz, *WIEN2k: An Augmented Plane Wave Plus Local Orbitals Program for Calculating Crystal Properties* (Vienna University of Technology, Austria, 2001).
[37]M. G. Brik, M. Piasecki, and I. V. Kityk, Inorg. Chem. **53**(5), 2645–2651 (2014).
[38]F. Bassani and G. P. Parravicini, *Electronic States and Optical Transitions in Solids* (Pergamon Press Ltd., Oxford, 1975), pp. 149–154.
[39]H. Tributsch, Z. Naturforsch. A **32A**, 972 (1977).
[40]D. R. Penn, Phys. Rev. B **128**, 2093 (1962).
[41]D. Xue, K. Betzler, and H. Hesse, Phys. Rev. B **62**, 13546 (2000).
[42]M. I. Alonso, J. Pascual, M. Garriga, Y. Kikuno, N. Yamamoto, and K. J. Wakita, Appl. Phys. **88**, 1923 (2000).
[43]A. H. Reshak, Ph.D. thesis, Indian Institute of Technology, Roorkee, India, 2005.
[44]A. H. Reshak, S. Auluck, and I. V. Kityk, Appl. Phys. A **91**, 451–457 (2008).
[45]K. Yoodee, J. C. Woolley, and V. Sa-Yakanit, Phys. Rev. B **30**, 5904 (1984).